14

Low Temperature Thermochemical Treatments of Austenitic Stainless Steel Without Impairing Its Corrosion Resistance

Askar Triwiyanto[1], Patthi Husain[1],
Esa Haruman[2] and Mokhtar Ismail[1]
[1]*Universiti Teknologi PETRONAS,*
[2]*Bakrie University,*
[1]*Malaysia*
[2]*Indonesia*

1. Introduction

Austenitic stainless steel (ASS) is used applied widely owing to its very good corrosion resistance. However, the application of this material as a bearing surface is severely limited by very poor wear and friction behaviour. Consequently, Surface Engineering treatments for austenitic stainless steel are an interesting alternative way to increase the surface hardness and improve the wear resistance. For the purpose of this works, the Surface Engineering design will be classified, very broadly, into three groups : (a) those which coat the substrate: PVD, CVD, etc, (b) those which modify only the structure of the substrate, (c) those which modify the chemical composition and the structure of the substrate: thermochemical, ion implantation, plasma, etc. It is nowadays widely accepted that hard, wear and corrosion resistant surface layers can be produced on ASS by means low temperature nitriding and/or carburizing in a number of different media (salt bath,gas or plasma), each medium having its own strengths and weaknesses. In order to retain the corrosion resistance of austenitic stainless steel, these processes are typically conducted at temperatures below 450^{o}C and 500^{o}C, for nitriding and carburizing respectively. The result is a layer of precipitation free austenite, supersaturated with nitrogen and/or carbon, which is usually referred to as S-phase or expanded austenite.

2. Enlarging application of Austenitic Stainless Steel

Starting from the mid of 1980's, investigations have been performed to improve surface hardness of ASS and thus enlarging their possibility of wider application, but led significant loss of its corrosion resistance. This tendency occur due to the sensitivity effect. Sensitization is a common problem in austenitic steel where precipitation of chromium carbides ($Cr_{23}C_6$) occurs at the grain boundaries at elevated temperatures, typically between 450 to 850^{o}C; diffusional reaction in forming chromium nitride/carbide leads to the depletion of Cr in the austenitic solid solution and consequently unable to produce Cr_2O_3 passive layer to make stainless feature. As a result, it reduces the corrosion resistance property of the stainless

steel. This phenomenon causes reduction in ductility, toughness and aqueous corrosion resistance (Clark & Varney, 1962).

The efforts have been made in the past decades to modify the surfaces of these materials to improve their surface hardness, wear resistance as well as corrosion resistance which is shown in Fig. 1.

Fig. 1. Enlarging application of Austenitic Stainless Steel (Czerwiec, 2010).

Bell et al. (T. Bell, 2001) suggested that a low temperature nitriding can eliminate the formation of chromium nitrides but at the expense of strengthening effects made by CrN precipitates. Alternatively, the strengthening effect will be replaced by supersaturation of interstitial species in austenite matrix which leads to the hardening of the surface region several tens micro meter thick. This precipitation-free nitride layer not only exhibits high hardness but also possesses good corrosion resistance due to the availability of retaining chromium in solid solution for corrosion protection.

In relation with the functional properties of a part, such as fatigue and static strength, or wear and corrosion resistance, are the basis for specifying the proper process and steel as illustrated in Fig. 2. (T. Bell, 2005). The functional part properties that essentially depend on the compound layer are wear resistance, tribological properties, corrosion resistance and general surface appearance. Both abrasive and adhesive wear resistance increase with hardness and with minimised porosity of the compound layer. Porosity can be positive in lubricated machinery parts as the pores act as lubricant reservoirs. The compound layer depth has to be deep enough not to be worn away. The diffusion layer (depth, hardness and residual stress) determines surface fatigue resistance and resistance to surface contact loads.

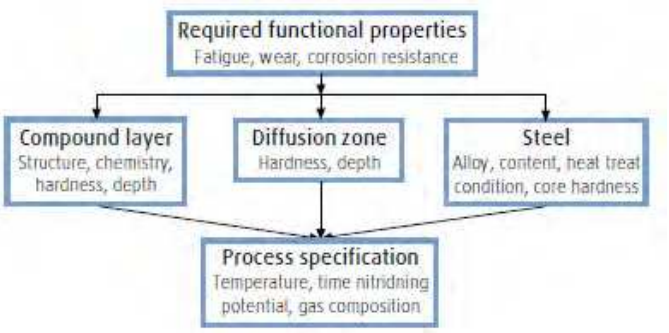

Fig. 2. The steps to process specification starting from required part properties.

2.1 Thermochemical and diffusion surface engineering treatments

Thermochemical treatments, sometimes referred to as case hardening or cementation, are based on the modification of the chemical composition of the substrate material. These treatments can be succeeded by a change in the structure through heat treatment. The formal definition available in BS EN 10052:1994 reads as follows (British standard, 1994):

Thermochemical treatment: Heat treatment carried out in a medium suitably chosen to produce a change in the chemical composition of the base metal by exchange with the medium.

In the case of diffusion treatment, the definition in that same standard is:

Diffusion treatment: Heat treatment or operation intended to cause the diffusion towards the interior of the ferrous product of elements previously introduced into the surface (for example, following carburizing, boriding or nitriding).

The two major low temperature thermochemical processes developed for austenitic stainless steels are nitriding and carburizing (Lewis et al, 1993; Bell. T, 2002). The former is normally carried out at temperatures below 450ºC and the later below 500ºC. The purpose of using low temperatures is to suppress the formation of chromium nitrides and carbides in the alloyed layers, such that chromium is retained in solid solution for corrosion protection (Sun et al, 1999; Thaiwatthana et al, 2002). Hardening of the nitrided layer and the carburised layer is due to the incorporation of nitrogen and carbon respectively in the austenite lattice, forming a structure termed expanded austenite, which is supersaturated with nitrogen and carbon respectively (Lewis et al, 1999; Thaiwatthana et al, 2002). More recently, a hybrid process has also been developed, which combines the nitriding and carburizing actions in a single process cycle by introducing nitrogen and carbon simultaneously into the austenite lattice to form a hardened zone comprising a nitrogen expanded austenite layer on top of a carbon expanded austenite layer (Tsujikawa et al, 2005; Sun et al, 2008; Li et al, 2010). There exist some synergetic effects between nitrogen and carbon: under similar processing conditions, the hybrid treated layer is thicker, harder and possesses better corrosion resistance than the individual nitrided layer and carburised layer.

From these definitions it becomes clear that two main factors will govern the process, namely: the exchange or absorption reaction with the medium, and the diffusion in the metal (ASM, 1977). As it is illustrated in Fig. 3, the medium will determine the way in which

the diffusing elements are delivered to the metal surface. A number of different media are available (solid, liquid, gas and plasma), and a detailed account of the media used for carburizing will be given in a following section.

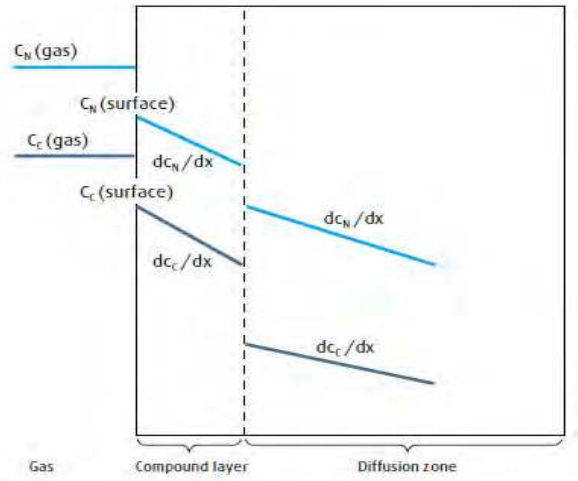

Fig. 3. Concentrations and concentration gradients of nitrogen and carbon. (Christiansen & Somers, 2005)

Once in the metal, the transport of the absorbed substance takes place by diffusion, and follows Fick's laws:

$$J = - D \, [dC/ dx] \tag{1}$$

$$J = - D \, [\partial C / \partial x] \tag{2}$$

$$\partial C / \partial t = [\partial^2 C / \partial x^2] / \partial x^2 \tag{3}$$

where J is the flux of diffusing substance, D is the diffusion coefficient, and $\partial C / \partial x$ is the concentration gradient (ASM, 1977). Therefore, the transport of the substance in solution is driven by its concentration gradient and the diffusion coefficient which, at the same time, depends on the temperature, the chemical composition and phase structure of the substrate. For a given alloy, kept at constant temperature in a medium with a consistent concentration of the substance of interest, the case depth will only depend on the time, according to equation (9):

$$x = a \, (Dt)^{½} = K t^{½} \tag{4}$$

where x is the case depth, a is a constant, D is the element diffusivity, t is the treatment time and K is a factor determined by a and D (ASM, 1977). Higher treatment temperatures yield the same case depth in shorter time, although there are technical limitations related with life of the furnaces, and metallurgical considerations regarding the side effects of keeping the substrate material at high temperatures (Parrish & Harper, 1994). Consequently, diffusion treatments are slower when compared to other surface deposition techniques (Hurricks,

1972), and treatments as long as 72 hours are common practice in industry. On the other hand, thermochemical treatments produce smooth case-core interfaces, which are beneficial for not only the wear and fatigue performance, but also the load bearing capacity (Sun & Bell, 1991).

During nitriding, ammonia (NH_3) in the furnace atmosphere decomposes into hydrogen and nitrogen at the surface, enabling nitrogen atoms to be adsorbed at the steel surface and to diffuse further into the steel as illustrated in Fig. 3. In nitrocarburizing it is additionally necessary to have a carbonaceous gas transferring carbon to the steel surface.

The flux of nitrogen and carbon from the gas to the steel surface is proportional to the concentration differences between the gas and the surface:

$$dm_N/dt_{(surface)} = k_1 [\, c_{N\ (gas)} - c_{N\ (surf)} \,] \tag{5}$$

$$dm_C/dt_{(surface)} = k_2 [\, c_{C\ (gas)} - c_{C\ (surf)} \,] \tag{6}$$

Here m denotes mass, t time, c concentration per volume unit and k_1 and k_2 are reaction rate coefficients.

The transfer of nitrogen and carbon from the surface further into the steel is controlled by diffusion. Diffusion rates follow Fick's first law, which for the compound layer and diffusion zone are respectively:

$$dm/dt_{(comp\ layer)} = - D_{Comp}\, dc/dx \tag{7}$$

$$dm/dt_{(diff\ zone)} = - D_{Diff}\, dc/dx \tag{8}$$

Balance of mass requires that all three mass transfer rates are equal:

$$dm/dt_{(surface)} = dm/dt_{(comp\ layer)} = dm/dt_{(diff\ zone)} \tag{9}$$

The slowest of the three stages controls the nitrogen and carbon transfer rates. For a compound layer consisting of alternating ε-γ′-ε layers, the rate will be determined by the phase with the slowest diffusion properties.

2.2 Diffusion in austenitic stainless steel

The mechanisms of nitriding and carburizing involve the transfer of the diffusing species to the surface, the establishment of a diffusing species activity gradient which drives the diffusion process, and the diffusion for itself, may be accompanied by the formation of nitrides or carbides (on the surface or in the core). The diffusion of interstitial species into a metal can only proceed if it exists a chemical potential (or activity) gradient of those species between the surface and the core of the material.

The first step of a thermochemical treatment therefore leads to enrichment of the treated substrate surface with active species. This process makes it necessary to decompose or activate (thermally or in plasma) the gaseous atmosphere and to bring the active species to the surface, so that they can be initially absorbed and afterwards diffuse into the substrate.

The diffusion of the nitrogen and/or carbon elements successively leads to the following steps: (i) the formation of a diffusion layer enriched with the diffusing elements and if the

solubility of the latter in the substrate is sufficient then this diffusion layer can be out of equilibrium at low temperatures (ii) at higher temperatures the follow steps occur. The surface formation of nitride, carbide or carbonitride layers of the main element of the substrate and (iii) the subsurface precipitation of nitrides, carbides or carbonitrides of alloying elements in the substrate (e.g. Fe, Ti, Al, Cr, Mo, V). In addition to the law of thermodynamics, the formation of the various phases is also govern by the nitrogen and carbon surface activities, and therefore are related to the temperature of the process used (gaseous or plasma), and to the composition of the gas.

Tables 1. (a) and (b) summarize the possible nitriding and carburizing configuration as described by Hertz, et al. (2008).

Substrate	N solubility	Potential nitrides	Compound layer+ diffusionlayer+ precipitation	Compound layer+ diffusion layer	Diffusion layer + precipitation	Diffusion layer only
Engineering steels	A little in α, more in γ	ε-$Fe_{2-3}N$ γ'-Fe_4N CrN, with alloys elements	Yes	Yes	Yes	Yes
Stainless steels	A little in α, more in γ	ε-$Fe_{2-3}N$ γ'-Fe_4N CrN, with alloys elements	Yes: but with reduced corrosion resistance	Yes	Not of industrial interest	Yes

(a)

Substrate	N solubility	Potential nitrides	Compound layer+ diffusion layer+ precipitation	Compound layer+ diffusion layer	Diffusion layer+ precipitation	Diffusion layer only
Engineering steels	A little in α, more in γ	Fe_3C, Cr–C, with alloys elements	Yes	Yes	Yes	Yes
Stainless steel	A little in α, more in γ	Fe_3C, Cr–C, with alloys elements	Yes: but with reduced corrosion resistance	Yes	Not of industrial interest	Yes

(b)

Table 1. Possible configurations of (a) nitriding, (b) carburizing.

To reduce further the potential of distortion and to avoid structural modifications of the substrate, and without repeating the quench and tempering treatments, these carburizing and nitriding treatments have evolved, in the past few years, towards lower temperature processes (350–450°C for austenitic stainless steels). This reduction in the treatment temperatures had to include specific treatments for removing oxide layers, which act as a barrier to the diffusion of nitrogen and carbon.

2.3 Diffusivity of simultaneous nitrogen and carbon in austenitic stainless steel

From diffusion experiments performed by Million et al, (1995), the interesting interactions of nitrogen and carbon are known, indicating that the presence of nitrogen enhances the activity of carbon and thus, its diffusion. It should, therefore, be possible to produce expanded austenite and to enhance the layer growth by simultaneous carbon and nitrogen

implantation. Treatment of austenitic stainless steel in either nitrogen or methane plasma at 400 ºC results in the formation of expanded austenite (Zhang et al, 1985 & Ueda et al, 2005). The different amounts of nitrogen or carbon in solid solution can be explained by the strength of the interaction between nitrogen or carbon and chromium. Williamson et al, (1994) noted that the strong interaction of nitrogen with chromium results in the trapping of nitrogen at chromium sites. This leads to a much higher supersaturation but reduced diffusivity in comparison to a methane treatment. However, the interaction is not really strong to form CrN. Carbon has a weaker interaction with chromium, so it diffuses inwards faster and a lower supersaturation is attained under similar treatment conditions. In both cases, nitrogen and carbon remain in solid solution, presumably on interstitial sites.

3. Thermochemical surface treatment to produce expanded austenite

As it has been known that the chemical composition of austenitic stainless steel makes them fully austenitic up to room temperature, and thus no phase transformation hardening takes place upon quenching. Consequently, surface treatments are an interesting alternative way to increase the surface hardness and improve the wear resistance. However, surface treatment of this steel has traditionally been considered bad practice (ASM , 1961), as it poses two main problems: the passive oxide film and the precipitation of chromium carbides (Sun et al, 1999). The passive chromium oxide film on austenitic stainless steel is stable under a wide range of conditions and isolates the substrate from the environment. This effect has been of interest for austenitic stainless steel components exposed to carburizing gas mixtures, either in service (Christ, 1998 & Yin, 2005) or for surface engineering purposes (Ueda et al, 2005). In the latter case, the oxide layer impairs diffusion of the hardening elements and, consequently, needs to be removed by applying some sort of surface activation process prior to the surface engineering treatment (Parascandola et al, 2001 & Sommers et al, 2004). Furthermore, traditional surface engineering treatments are conducted at high temperature, around 500–600 ºC in the case of nitriding, and 900–1000 ºC for carburizing (Zhang et al, 1985 & Ueda et al, 2005). At these temperatures, and with increasing availability of nitrogen and carbon from the hardening medium, profuse precipitation of chromium nitrides and carbides occurs, leading to a marked deterioration of the corrosion resistance of Austenitic stainless steel. However, low temperature thermochemical diffusion treatments with nitrogen and/or carbon have been reported to increase the surface hardness without affecting or even improving the corrosion resistance (Bell. T & Sun, 1998).

The most popular technology used to achieve the aforementioned low temperature thermochemical treatments of stainless steels is plasma technology, namely plasma nitriding (Rie & Broszeit, 1995; Stinville et al, 2010), plasma carburizing (Sun, 2005, Tsujikawa et al, 2007) and plasma hybrid treatments (Sun, 2008; Li et al, 2010). Due to the formation of a native oxide film stainless steel surface when exposed to air or residual oxygen before and during the treatment process, it is rather difficult to facilitate nitrogen and carbon mass transfer from the treatment media to the component surface. However, during plasma processing, due to the sputtering effects of energetic ions, the oxide film can be removed easily and effective mass transfer is obtained. This makes the plasma technology unique for surface treatment of stainless steels. An alternative is using the more conventional gaseous processes like gas nitriding (Gemma et al, 2001) and gas carburizing (Ernst et al, 2007).

These have proven feasible and industrially acceptable for performing low temperature nitriding and carburizing of stainless steels, provided that the component surface is activated before the gaseous process by special chemical treatments and the oxide film formed during the gaseous process is disrupted by introducing certain special gas components (Gemma et al, 2001).

Fluidized bed as one method of thermochemical surface treatments could employed as the expanded austenite (EA) layer formation on source of interest. To obtain the structure, thickness and and quality of the alloyed zone of γ_N and γ_C can be controlled by the processing parameters, such as temperature, time and gas composition in the fluidized bed. The duplex surface layer by combined carburizing and nitriding of 316L steel should be thick and mildly dropping hardness profile. Focusing in the concentration of hybrid process in terms of surface morphology, elemental profiles/structural characteristics, hardness and tribological properties, and corrosion behavior were placed in this presentation.

The use of fluidized bed furnace in heat treating operation has been introduced by Reynoldson which offers several advantages, including faster treatment time, precise control of treatment parameters, despite its economic benefits of low investment and operational cost (Reynoldson, 1995; Haruman & Sun, 2005). The schematic picture of fluidized bed furnace is shown on Fig. 4. Recent work has shown that low temperature nitriding of austenitic stainless steel is possible in a fluidized bed furnace (Haruman & Sun, 2005).

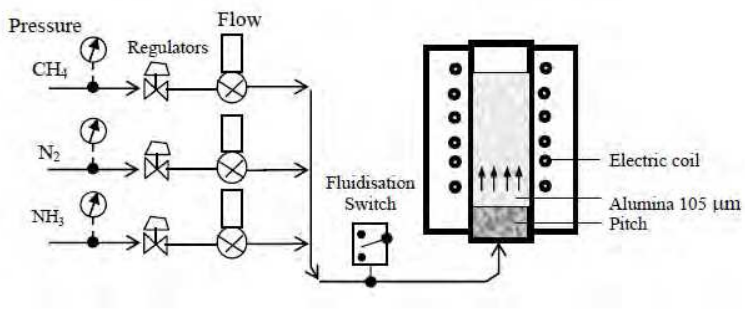

Fig. 4. Schematic picture of Fluidized bed furnace.

It is nowadays widely accepted that hard, wear and corrosion resistant surface layers can be produced on Austenitic stainless steel by means low temperature nitriding and/or carburizing in a number of different media (salt bath, gas or plasma), each medium having its own strengths and weaknesses (Bell, 2002). In order to retain the corrosion resistance of austenitic stainless steel, these processes are typically conducted at temperatures below 450 ^oC and 500 ^oC, for nitriding and carburizing respectively. The result is a layer of precipitation free austenite, supersaturated with nitrogen and/or carbon, which is usually referred to as S-phase or expanded austenite (Sun et al, 1999; Li, 2001; Li, et al., 2002; Christiansen, 2006).

Expanded austenite is the microstructural feature which responsible for the highly demanded combination of excellent corrosion and wear performances. Expanded austenite γ_X (X = N, C) hitherto also called S-phase (Ichii et al, 1986; Thaiwatthana et al, 2002;

Christiansen et al., 2004). Expanded austenite without nitrides/carbides is obtained when high amounts of atomic nitrogen and/or carbon are dissolved in stainless steel at temperature below 450 °C for nitrogen and about 550 °C for carbon. The nitrogen/carbon atoms are presumed to reside in the octahedral interstices of the f.c.c. lattice (Christiansen et al, 2004). Long range order among the nitrogen/carbon atoms has so far not been confirmed with X-ray diffraction techniques. Typically, nitrogen contents in expanded austenite range from 20 to 30 at% N; carbon contents range from 5 to 12 at% C (Sun et al, 1999 & Blawert et al, 2001). In terms of N:Cr ratio the homogenity range of nitrogen-expanded austenite spans from approximately 1:1 to 3:1 (Christiansen & Somers, 2005). Expanded austenite is meta-stable and tends to develop chromium nitrides/carbides (Li et al, 1999; Jirásková, et al., 1999; Christiansen & Somers, 2005,). The high interstitial content of C/N is obtained because of the relatively strong affinity of Cr atoms for N and (to a lesser extent) C atoms, leading to anticipated short range ordering of Cr and N/C. Due to the low mobility of Cr atoms as compared to interstitial N/C atoms at lower treatment temperatures, chromium nitrides/carbides do not precipitate until after long exposure times and N/C is kept in solid solution by the Cr "trap sites".

The improvement in wear resistance is perhaps the most outstanding feature of EA. The degree of improvement depends on the sliding conditions, but volume losses between one and two orders of magnitude lower than the untreated ASS are commonly reported for dry sliding (Thaiwatthana et al, 2002). This improvement is attributed to the increased surface hardness, with a typical ratio 4:1 compared to the untreated ASS (Qu et al, 2007). The EA layer prevents the surface from undergoing plastic deformation, and changes the wear mechanism from adhesion and abrasion, to a mild oxidational wear regime (Qu et al, 2007). However, under heavier loads, deformation of the subsurface occurs and leads to catastrophic failure, through propagation of subsurface cracks and spallation of the EA layer (Sun & Bell, 2002). In this way, the carbon EA layers, being thicker and tougher than their nitrogen counterparts, show some advantage.

With regard to corrosion, the results vary significantly depending on the testing conditions. Surprisingly, most researchers found that low temperature nitriding and/or carburizing do not harm the corrosion resistance of ASS, or even improve it. No conclusive explanation has been found for this improved corrosion behaviour, although it is clear that the benefit stands as long as nitrogen and carbon remain in solution and EA is free of precipitates (Li & Dong, 2003). In NaCl solutions, it is generally reported that EA remains passive under similar or wider range of potential compared to the untreated ASS, carbon EA showing a marginal advantage over nitrogen EA (Martin et al, 2002). Similar or slightly higher initial current densities have usually been measured on EA, together with the absence of pitting potential, in contrast to what is usual for ASS (Aoki & Kitano, 2002). Regarding repassivation, the evidence indicates that the passive film heals slower on EA than on ASS (Dong et al, 2006).

3.1 The influence of process variables and composition of expanded austenite

The depth profiles for thermochemically hardened stainless steels typically show a trend of increasing depth with higher temperatures and longer process durations. The very hard layer of nitrogen-expanded austenite exhibits a relatively shallow depth with an abrupt transition to the softer substrate material. The high hardness values associated with nitrided

layer formation are consistent with the large compressive stresses in the residual stress profiles which were determined by XRD.

Previous investigation which regards to the influence temperature and time of thermochemical treatments using Fluidized bed shows that nitriding at 400°C for times up to 6 h could not produce a continuous nitrided layer on the substrate surface. When temperature was increased to 450°C, a uniform layer was formed after 6 h nitriding and was not effective for shorter treatments due to only a very thin discontinuous layer formation after 3 h nitriding, whilst after nitriding for 6 h a layer about 13 μm thick was formed, which has a bright appearance and is resistant to the etchant used to reveal the microstructure of the substrate. Increasing the temperature to 500°C resulted in the formation of a relatively thick nitrided layer after 3h and 6 h nitriding. The morphology of the nitrided layers formed at this temperature for longer treatment times is different from that formed at 450°C for 6h. Some dark phases were formed in the layers which is similar to those observed for plasma nitrided product and can be attributed to the decomposition of the S phase and the formation of chromium nitrides, which is believed reduce the corrosion (T. Bell, 1999).

The microhardness measurement on the nitrided subtrate showing a function of processing time for the three different temperatures. It can be concluded that no obvious hardening was achieved after nitriding at 400°C. The hardening effect is also insignificant after nitriding at 450°C for 1 h and 3h, and at 500°C for 1h. This corresponds well with the above metallographic examinations that no effective nitriding was achieved under these conditions.

According to these, both structural analysis and hardness measurement indicate that under the fluidized bed nitriding conditions, there exists an incubation time for the initiation of nitriding reactions. Nitriding must be carried out for a duration longer than the incubation time in order to produce an effective nitrided layer. From the experimental results, it is also evident that the incubation time is temperature dependent: increasing nitriding temperature reduces the incubation time.

This incubation time phenomena, which has not been reported for other nitriding processes, such as plasma nitriding, may be related to the nature of the fluidized bed process, where the disruption of the native oxide film on the specimen surface, which is required to effect the nitriding reactions, has to rely on thermal dissociation. The higher the temperature, the faster is the dissociation of the oxide film and thus the shorter the incubation time.

4. Experimentals method

The substrate material used in this work was AISI 316L type austenitic stainless steel of following chemical compositions (in wt.%): 17.018 Cr, 10.045 Ni, 2.00 Mo, 1.53 Mn, 0.03 C, 0.048 Si, 0.084 P, 0.03 S and balance Fe. This steel was supplied in the form of 2 mm thick hot-rolled plate. Samples of 20 mm x 70 mm size rectangular coupon were cut from the plate. The sample surface was ground on 320, 600, 800, 1000, 1200 grit SiC papers, and then polished using 1 μm Al_2O_3 pastes to the mirror finish. Before treating, these specimens were cleaned with acetone. The treatments were performed at 450^{o}C for a total duration of 8 hours in an electrical resistance heated fluidized bed furnace having 105 μm particulate alumina as fluidized particles which flow inside the chamber due to the flow of nitriding or

carburizing gases. The fluidized bed furnace, which was manufactured by Quality Heat Technologies Pty Ltd has a working chamber of 100mm diameter x 250mm deep with maximum worksize of 70mm diameter x 150mm high. Before charging the samples, the chamber was heated to the treatment temperature of 450oC with the flow of nitrogen gas at 1.05 m^3 per hour. Then the samples were charged to the furnace and the treatment gases were introduced and their flow rates were adjusted to meet the required composition, with the total gas flow rate maintained at 0.62 m^3 per hour. Table 2. summarizes the process conditions employed in this work. Four different treatments were conducted, including low temperature nitriding, carburizing, hybrid process, and sequential carburizing-nitriding. The hybrid process involved treating the sample in an atmosphere containing both NH_3 (for nitriding) and CH_4 (for carburizing) for a total duration of 8 h, whilst the sequential process involved treating the sample in the carburizing atmosphere for 4 h and then in the nitriding atmosphere for further 4 h.

Nitriding, carburizing, and hybrid treatments were performed at 450°C in a fluidized bed furnace having particulate alumina as fluidized particles which flow inside the chamber due to the flow of nitriding or carburizing gases.

	Symbol	Temp. (°C)	Gas (%)			Time	Temp.(°C)	Gas (%)			Time	Layer Thickness (μm)
			CH_4	N_2	NH_3			CH_4	N_2	NH_3		
Nitriding	**8N**	450°		85	15	8	No treatment	0	0	0	No treatment	8,35
	5N	450°		85	15	5	No treatment	0	0	0	No treatment	5,10
	2N	450°		85	15	2	No treatment	0	0	0	No treatment	3,26
Carburising	**8C**	450°	5	95		8	No treatment	0	0	0	No treatment	3,92
	5C	450°	5	95		5	No treatment	0	0	0	No treatment	1,63
	2C	450°	5	95		2	No treatment	0	0	0	No treatment	1,20
Nitrocarburising	**8(C+N)**	450°	5	80	15	8	No treatment	0	0	0	No treatment	4,00
	5(C+N)	450°	5	80	15	5	No treatment	0	0	0	No treatment	2,16
	2(C+N)	450°	5	80	15	2	No treatment	0	0	0	No treatment	1,25
		First Step					Second Step					
Hybrid	**4C-4N**	450°	5	95		4	450°		85	15	4	5.2
	2C-3N	450°	5	95		2	450°		85	15	3	1.6
	1C-1N	450°	5	95		1	450°		85	15	1	1.37

Table 2. Treatment conditions and their corresponding layer thicknesses.

The specimens were heated by electrical resistance heating. Prior to treating, the specimens were soaked in concentrated HCl (2 M) solution for 15 minutes duration with the purpose to remove the native oxide film that commonly forms on austenitic stainless steel and protects the metal matrix from corrosion. This oxide layer is believed to act as a barrier for diffusional nitrogen transport (Rie, 1996). After thermochemical treatments, the specimens were quenched in water. The treated specimen cross sections were first characterized by metallographic examination. To reveal the microstructure, the polished surface was etched

in Marble's solution (4 g $CuSO_4$ + 20 ml HCl + 20 ml distilled water). The schematic picture of fluidized bed furnace is shown on Fig. 4.

The specimens were further characterized by microhardness indentation, elemental analysis by FESEM and X-ray diffraction (XRD) analysis using Cu-Kα radiation. Tribological properties were evaluated with a Taber® Linear abraser model 5750 dry slide tribo-tester using an 5-mm diameter AISI 316L collet nut as mate material. The stroke length applied was 25.4 mm under a constant load 600 g. After 3600 cycles of sliding (completed in 60 minutes) having maximum velocity of 79.76 mm/sec, the specimen wear loss was measured by balance to evaluate cumulative weight loss. Microstructures of treated layers were investigated by X-Ray diffraction analysis (XRD) using Cu-Ka (40 kV, 150 mA) and Field Emission Scanning Electron Microscopy (FESEM). The electrochemical corrosion behaviour of the as-treated surfaces was evaluated by measuring the anodic and cathodic polarisation curves in aerated 3.0 % NaCl solution at a scan rate of 1 mV/min. The tests were conducted at room temperature by using a three electrode potentiostat with a computer data logging, requisition and analysis system. Potentials were measured with reference to the standard calomel electrode (SCE).

Corrosion tests were performed electrochemically at room temperature in a flat cell with 3.0% NaCl in distilled water. The flat cell, as schematically shown in Fig. 5, was a three-electrode set-up consisting of a saturated calomel reference electrode (SCE), a platinum auxiliary electrode and a working electrode (sample). Sample to be tested was placed against a Teflon ring at one end of the flat cell, leaving a theoretical circle area of 67.5 mm^2 on the sample surface in contact with the testing solution through a round hole in the Teflon ring. Test control, data logging and data processing were achieved by a ''Sequencer'' computer software. The scanning potential was in the range of -0.5 to + 1.4 V, and the scan rate was 1 mV/s. From the polarization curves, the average values of the corrosion potential (E_{corr}), the corrosion current density (I_{corr}) and the polarisation resistance (LPR) were calculated.

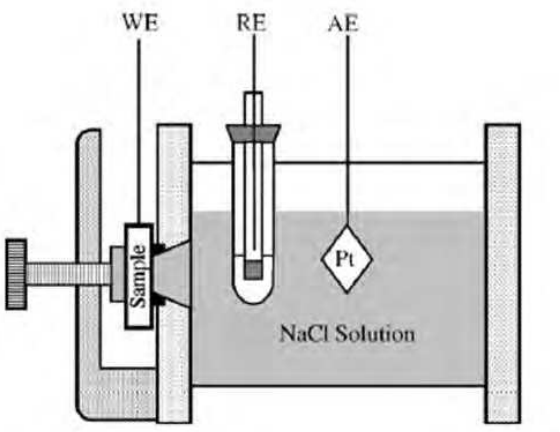

Fig. 5. Schematic diagram of the flat cell used for polarization corrosion test (Li & Bell, 2004).

5. Key results

5.1 Layer morphology and hardness profile

Hardened layers with different morphologies were observed as a result of the various treatment conditions and the thicknesses of the layers produced in different conditions are shown in Table 2. The layer thicknesses are found to be different at different treatments, and their growths against time in Fig. 6. show that layer thickness increases with processing time.

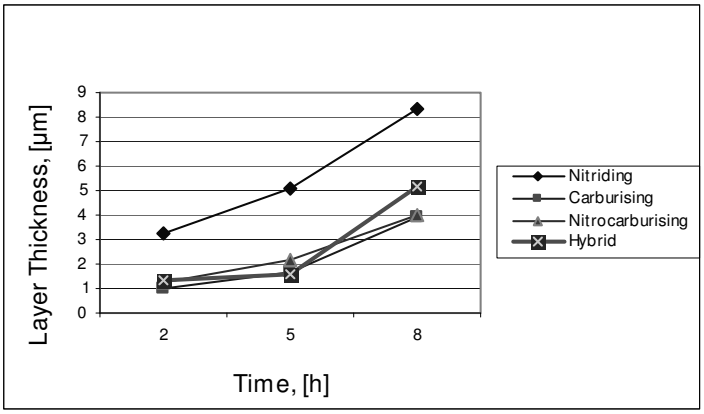

Fig. 6. Thickness of treated layers measured from micrographs.

Micrographs in Fig. 7 show that the morphology of the layer changed with treatment conditions. The two specimens processed under combined treatment conditions, 8(C+N), and 4C–4N produced duplex layers irrespective of whether they were processed simultaneously (Fig. 7b) or sequentially (Fig. 7d). The processed layer thicknesses in Table 2. show that the nitrided specimen, 8N, has a thickness between 3.26 to 8.35 µm and the carburized specimen, 8C, is in between 1.00 to 3.92 µm.

Furthermore, the nitrided-only 8N specimens have deeper layers than combined processed specimens. The depth of the simultaneously carburized and nitrided specimen, 8(C+N), reaches only 50% that of the nitrided specimen, and the thickness of 4C–4N specimen had only about 45% compared to the nitrided-only 8N specimen after being processed for the same duration of 8 h due to the half nitriding duration.

For a similar treatment duration, the Plasma process is reported by Tsujiwaka on 2005 which is produce about 18 µm thick layer which is much higher compared to that of the present conventional nitriding treatment in fluidized bed furnace. In plasma process the native oxide layer is removed mostly by bombardment of the plasma gas which is completely absent in conventional fluidized process. This is one of the reasons why convention fluidized bed treatment produced small layer thickness compared to the corresponding plasma nitriding. Previous investigation revealed that nitriding at 450°C became effective after treatment for 6 h where a continuous nitrided layer was produced (Sun, 2006). This is due to the fact that the incubation time phenomena which may be related to the nature of

the fluidized bed process, where the disruption of the native oxide film to cause the nitriding reactions, has to be by thermal dissociation. The higher the temperature, the faster is the dissociation of the oxide film and thus the shorter the incubation time. According to this hypothesis it is understood why a very thin discontinuous layer was formed after a 2 h treatment time ; the layer was about 8 μm thick after 8 h nitriding, which gave a bright appearance and was resistant to the etchant used to reveal the microstructure of the substrate. The treated layers for 4C-4N consist actually of two separate zones with a somewhat diffused interface which was clearly observed under microscope, but not revealed in the micrographs. The outer zone is γ_N and the inner zone is γ_C. Conversely, the nitrocarburised sample shows a distinct separation of the γ_N and γ_C layers, with the γ_C layer closest to the austenite substrate (as indicated in the micrograph in Fig. 7b). The X-ray diffractograms of carburised and nitrided AISI 316L show that two different types of expanded austenite are present (Fig. 6).

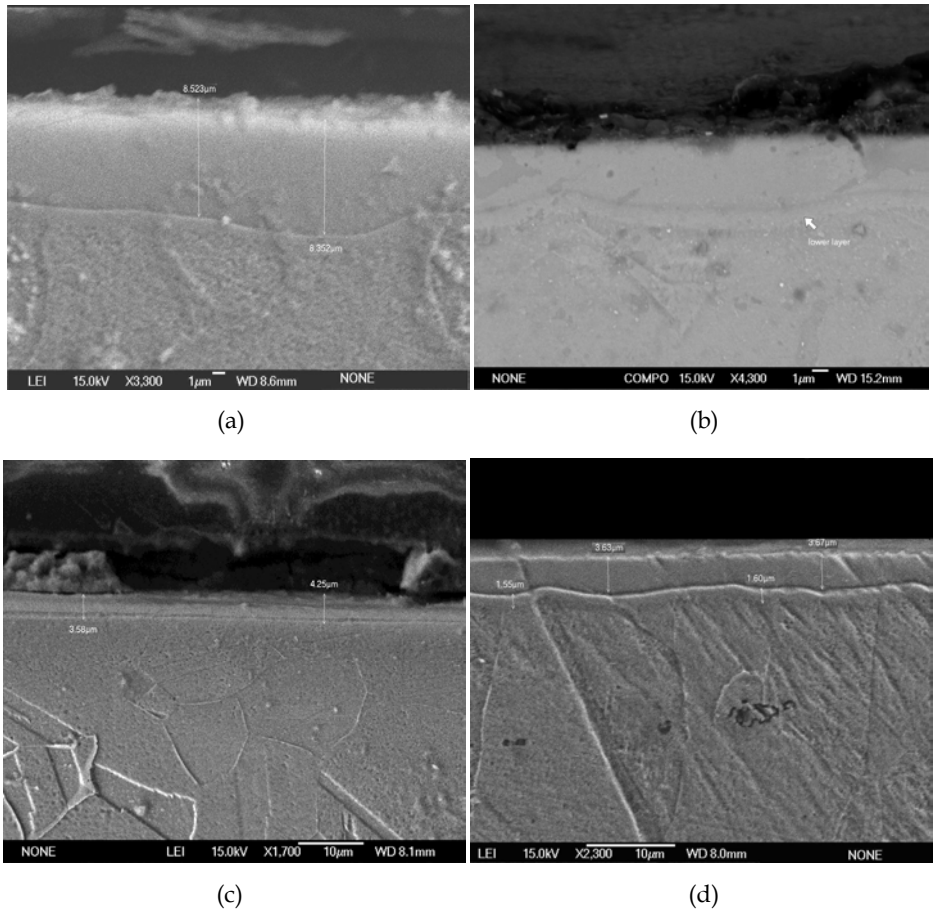

(a) (b)

(c) (d)

Fig. 7. SEM micrographs of 450°C treated specimens: (a) Nitrided 8 h, (b) Nitrocarburised 8 h, (c) Carburised 8 h, (d) Hybrid 4 h Carburised followed by 4 h Nitrided.

Fig. 8 shows the hardness depth profiles of the treated specimens. The carburized 8C specimen developed a maximum hardness of about 500 Hv, which is much lower than the hardnesses of 1230 to 1588 Hv for other three nitrided and nitrocarburised specimens. The nitrided layer of the 8N specimen produced a hard layer of 1588 Hv with an abrupt layer–core interface, while the 8C carburizing produced a gradually decreased hardness profile. Two combined carburized and nitrided specimens, 8(C + N) and 4C–4N developed a similar tendency to bulge in hardness profiles at inner carburized layer as shown in Fig. 7. The most gradual decrease in hardness from 1230 Hv level to substrate hardness was displayed by the 4C–4N specimen.

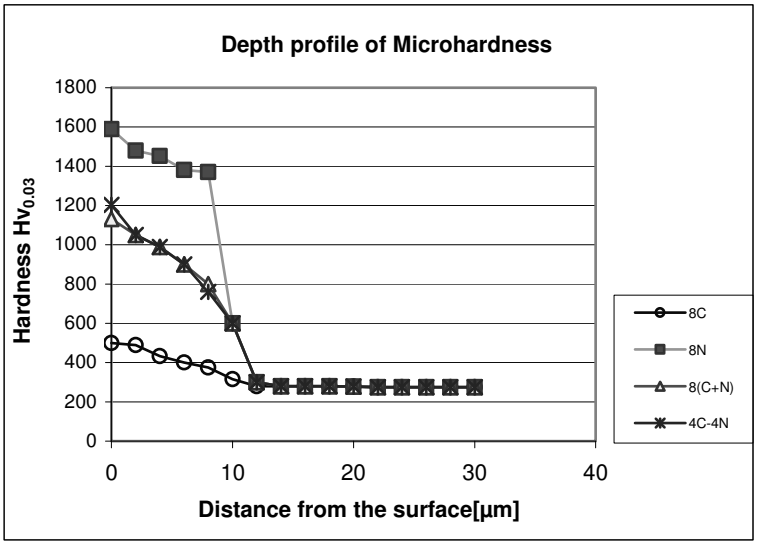

Fig. 8. Depth profiles of Microhardness.

5.2 Elemental profile of carbon and nitrogen

The carbon profile investigated on 4C-4N specimen using EDS FE-SEM is depicted in Fig. 9. It is found that higher carbon at the deeper layer which indicates that carbon pushed-ahead by the incoming nitrogen atom and the dissolved carbon is accumulated at the front of the nitride layer which has also been reported in the literature (Lewis et al, 1993).

Elemental analysis of the Hybrid specimen CN gave more carbon beyond the nitrided layer, but some carbon was also observed at the surface. The variations of chemical concentration in the hybrid nitrocarburized layer were also measured with EDS. These figures shows the typical nitrogen and carbon profiles produced in treated 316L steel. It can be seen from these Figures that there are two features in the nitrogen and the carbon profiles. Firstly, the nitrogen profile on the surface of the treated layer is similar to that of nitrided 316L steel. Secondly, the maximum nitrogen concentration is on the surface and the maximum carbon concentration appears beneath as if carbon was 'pushed' to the middle of the layer by nitrogen.

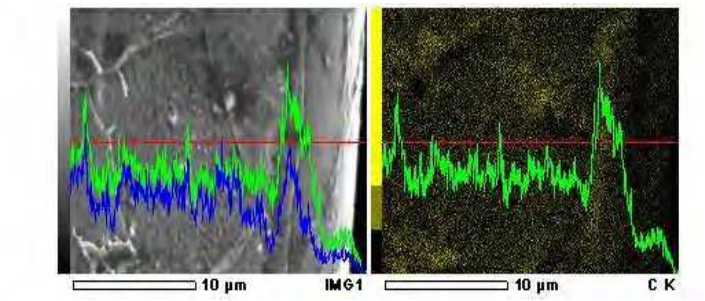

(a)

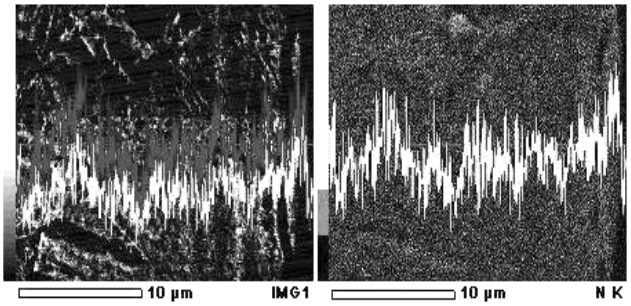

(b)

Fig. 9. Carbon profiles (a) and nitrogen profiles (b) along the depth.

Such distributions of nitrogen and carbon in the surface layer are likely to produce some beneficial influences upon the properties of hybrid treated 316L steel. Figure 6b shows results of nitrogen concentration on hybrid dual-stages obtained from energy dispersive X-ray (EDS) analysis. According to these curves, it can be clearly seen that the surface hybrid layer contains very high amount of nitrogen, and nitrogen concentration is gradually reducing from surface to the core with distance increasing due to a low diffusion rate in the case of samples at low temperature. However, some carbon remains in the sub-surface layer.

Fig. 10 summarizes the phase compositions in the treated specimens as determined by XRD from the specimen treated at 450°C for 8h. As confirmed by XRD analysis in Fig. 10, the nitriding treated surface layer comprises mainly the S phase or the expanded austenite. For the hybrid process, consisting of dual layers (Figs. 7d & 7e), revealed another thin interfacial layer. This interfacial layer is believed to be due to the accumulation of carbon as has also been reported in literature (Sun, 2006). One interesting aspect of the diffraction displayed in Fig. 10 regards the variation of the (200) diffraction line width in relation with 2θ angle. This behaviour can be explained by the lattice distortion caused by the greater amount of nitrogen in the interstitial sites and/or only by crystallographic orientation present in this phase. The XRD analysis did not show any peak from nitride or carbide phase.

In accordance with the findings for plasma nitriding (Lewis, 1993; Rie, 1995), the S phase layer produced in this fluidized bed furnace process has minimal chromium nitride/carbide precipitation. Comparing the diffractograms for the nitrided samples with the untreated material, it clearly shows that Bragg reflections (peaks) are shifted to lower 2θ angles. It was

caused primarily by the dissolution of nitrogen which causes a dilation of the fcc lattice (hence the name expanded austenite), although residual stress and stacking faults also play a role in this respect (Somers, 2005). The X-ray diffraction pattern of carburised AISI 316L is shown in Fig. 10. γ_C is identified as the only phase present in the surface adjacent region, i.e. within the information depth for the probing X-ray beam. A marked difference is observed as compared to nitrided AISI 316L; a smaller shift of the austenite peaks to lower 2θ, which indicates a substantially lower content of the interstitially dissolved atoms, provided that nitrogen and carbon induce a similar distortion in the fcc lattice. The asymmetrical (200) austenite peak in Fig. 10 indicates a depth-gradient of the carbon content in the near surface zone. The distinct peaks for the carburised sample indicate a smooth concentration gradient and lower defect density in γ_C layers as compared to γ_N layers.

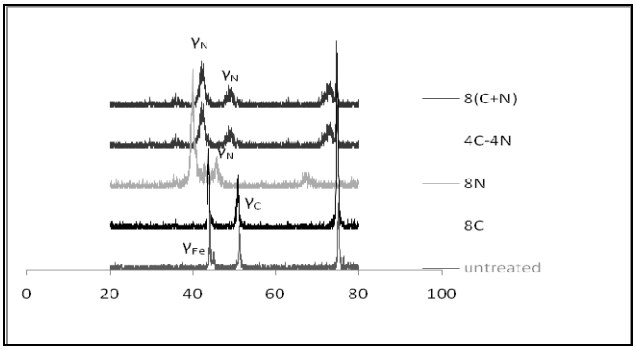

Fig. 10. Comparison of XRD patterns of treated specimens.

5.3 Wear property

The wear properties of the low temperature surface treatment specimens as weight loss under dry sliding friction are presented in Fig. 11 along with an untreated specimen for comparison purpose. The results suggest that the fluidized bed thermochemical-treated specimens have excellent wear resistance. The 8N specimen has the highest wear resistance compared to the values of 4C-4N, 8(C+N), and 8C specimens.

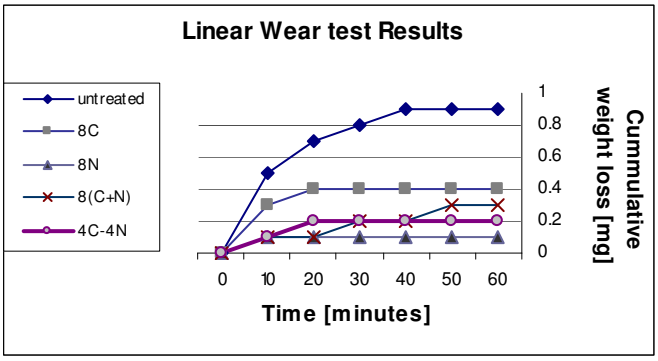

Fig. 11. Wear under dry sliding condition.

The highest hardness for 8N specimen is considered to be responsible for best wear resistance property among the treated specimens used in this investigation. However the findings suggest that nitriding, hybrid, nitrocarburizing and carburizing the austenitic stainless steel at 450^0C using a fluidized bed furnace can improve surface hardness and wear resistance of austenitic stainless steel. It is to be noted that at the initial stage of sliding, all the specimens in Fig. 11 gave accelerated weight loss and then leveling off after certain period. It is presumed that at the initial stage of sliding, the 600g load of the sliding mate material was encountered by the asperities of substrate surface, which effectively caused high load sliding and thus more wear loss. The eventual dropping off may be related to smoothening of the asperities at the wear surface, which produced more contact area for the sliding load of 600g and hence reduced or constant wear rate.

The work hardening effect may also cause this tendency together with possibilities of surface oxide or carbide/nitride formation at a certain period of sliding, thus leading to an equilibrium condition of constant wear rate. However, no evidence is available to explain the exact reasons of these wear phenomena.

5.4 Corrosion properties

Corrosion tests using the electrochemical technique demonstrated that the precipitation free carburized and nitrided layers have very good corrosion resistance in the corrosive environments.

The most subtantial improvement in properties of austenitic stainless steels by the hybrid process lies in corrosion resistance as evaluated by electrochemical testing (Li & Bell, 2004). Fig. 12 shows the anodic polarization curves measured for several specimens in 3.0% NaCl solution. As expected, both individual nitriding and carburizing reduce the current density of the steel in the anodic region, indicating improved corrosion resistance. After the hybrid treatment, the anodic polarization curve is shifted towards lower current density by several orders of magnitude as compared to that for the untreated and individually nitrided and carburised steel. This registers an improvement in corrosion resistance by several orders of magnitude and signifies the excellent corrosion resistance of the hybrid treated surface. The much enhanced corrosion resistance observed for the hybrid treated surfaces may be attributed to the extremely large supersaturation of the upper part of the nitrogen-enriched layer with both nitrogen and carbon (see Fig. 9). This would contribute to the observed higher hardness and better corrosion resistance as compared to those achieved by individual nitriding and carburizing.

The treatment conditions are the same as those in Fig. 7. The electrochemical test results for Hybrid-NCT, Nitriding-NT, Carburizing-CT were described in Fig. 12. The NT and CT showing that the current density of treated stainless steel were decreased in the anodic region which indicating positive effect regarding the improvement of corrosion resistance compared to the substrate. After Hybrid-NCT treatment, the anodic polarization curved is shifted towards lower current density which explain that the corrosion rate was decreased and the polarization current measurement gave 0.00003 mA/cm^2 and demonstrate an improvement in corrosion resistance as compared to that untreated and individually nitrided and carburized steel, while passivation current of NCT is the lowest followed by CT, NT and untreated respectively. This trend also similar to the maximum potential passivation behaviour since the

dissolution current density increased slowly and gradually with applied potential (Y. Sun & E. Haruman, 2008). Although in the first 250 mV/SCE scan of CT show small increases in current densities where the re-passivation behavior start to occur.

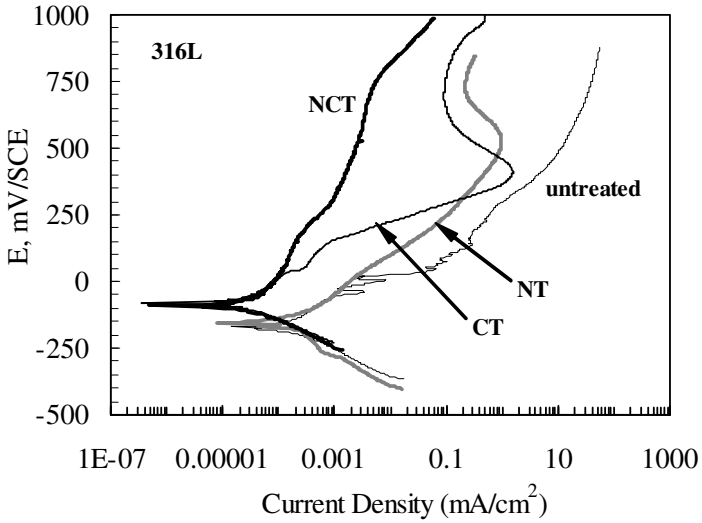

Fig. 12. Anodic polarization curves measured in 3.0%NaCl.

Although, the corrosion behaviour of low temperature nitrided, carburized and hybrid stainless steel thermochemical treatment have been investigated by several investigators (Zhang et al, 1985; Rie et al, 1995; Sun et al, 1999), the reason for improvement of corrosion resistance due to nitrogen and carbon supersaturation in austenite has not been fully understood. A possible mechanism is that supersaturation of nitrogen and carbon promotes the improvement of the passivation ability of austenite, and this effect seems to give beneficial with increasing degree of supersaturation (Munther et al, 2004). Thus, the improvement of corrosion resistance for hybrid-NCT treated material may be attributed to the extremely large supersaturation of the upper part of nitrogen-enriched layer with both nitrogen and carbon. This would be contribute to the observed higher hardness and better corrosion resistance as compared to those achieved by individual nitriding-NT and carburizing-CT.

6. Conclusion

The thermochemical treatments of AISI 316L stainless steel in a fluidized bed process at 450°C demonstrate that it is possible to produce hard layer of an expanded austenite phase without precipitation of chromium carbide/nitride. For nitriding and carburizing treatments the expanded layers consisted of a single layer γN or γC phase while specimens treated by nitrocarburizing or hybrid process gave dual layers consisting of γN at the surface and γC ahead of γN. The layer produced in fluidized bed process is not uniform in thickness under the same treatment conditions. The nitriding treatment produced 8.35 μm

thick layers after 8 h duration while carburizing and nitrocarburizing gave much smaller thicknesses for the same processing time. However the layer thickness is found to increase with the treatment time for all the processes. The nitrided treatment developed the highest hardness of 1600 Hv; 1150 Hv and 500 Hv was found for the nitrocarburised and carburized specimens, respectively. All treated specimens gave very good wear resistance compared to the untreated specimen; however, the nitrided specimen produced very high wear resistance which corresponds to highest hardness among the specimens tested. Thermochemical surface treatments of 316L were capable to produce expanded austenite layers which considerably improved the corrosion properties of 316L austenitic stainless steel. The electrochemical test results show that hybrid–NTC can significantly improve the corrosion resistance of austenitic stainless steel which is much better than that measured for the untreated stainless steel and the individually nitrided-NT and carburized-CT layers.

7. References

Akita, M. and Tokaji, K.: *Effect of carburizing on notch fatigue behaviour in AISI 316 austenitic stainless steel*, Surface and Coatings Technology (2006) 200, 20-21, 6073-6078

Aoki, K. and Kitano, K.: *Surface hardening for austenitic stainless steels based on carbon solid solution*, Surface Engineering (2002) 18, *6,* 462-464

C.X. Li and T.Bell, Corrosion Science 46, pp. 1527-1547 (2004).

Ceschini, L. and Minak, G.: *Fatigue behaviour of low temperature carburised AISI 316L austenitic stainless steel*, Surface and Coatings Technology (2007) 202, *9,* 1778-1 784

Clark. D.S. and Varney. W.R., Physical Metallurgy for Engineers, Litton educational publishers, (1962).

Committee on gas carburizing, A. S. M.: *Carburizing and carbonitriding*, 1st Ed. (1977) Metals Park, Ohio, American Society for Metals

D. B. Lewis, A. Leyland, P. R. Stevenson, J.Cawley and A. Matthews, Metallurgical study of low-temperature plasma carbon diffusion treatments for stainless steels, *Surf. Coat. Tech*. 60 (1993) 416-423.

D. Munther, H.-J. Species, H. Biermann, Chr. Eckstein, Trans. Mater. Heat Treat. 25 (5) (2004) 311-315.

Dong, H., Qi, P.-Y., Li, X. Y. and Llewellyn, R. J.: *Improving the erosion-corrosion resistance of AISI 316 austenitic stainless steel by low-temperature plasma surface alloying with N and C*, Materials Science and Engineering A: Structural Materials: Properties, Microstructure and Processing (2006) 431, 137-145

E. Haruman and Y. Sun, Proc. 3rd Asian Conf. on Heat Treat. of Mater., Gyeongju, Korea, 10-12 Nov, 2005.

E. Haruman, Y. Sun, H. Malik, A.G.E. Sutjipto, S. Mridha, K. Widi, Low Temperature Fluidized Bed Nitriding of Austenitic Stainless Steel, *Solid State Phenomena.*, Vol. 118, pp. 125-130, 2006.

F. Borgioli, A. Fossati, E. Galvanetto and T. Bacci, "*Glow-discharge nitriding of AISI 316L austenitic stainless steel: influence of treatment temperature*", Surfaces and Coatings Technology, 200, 2474 - 2480, (2005).

F. Ernst, Y. Cao, G.M. Michal, A.H. Heuer, Carbide precipitation in austenitic stainless steel carburized at low temperature, *Acta Mater*. 55 (2007) 1895-1906.

Hertz, et al., (2008) Technologies for low temperature carburizing and nitriding of austenitic stainless steel, *International Heat Treatment and Surface Engineerng,* vol. 2, No. 1.

Hurricks, P. L.: *Some aspects of the metallurgy and wear resistance of surface coatings*, Wear (1972) 22, *3,* 291-319

J. Qu, P. J Blau and Jolly, B. C.: *Tribological properties of stainless steel treated by colossal carbon supersaturation*, Wear (2007) 263, 1-6, 719-726

J.C. Stinville, P. Villechaise, C. Templier, J.P. Riviere, M. Drouet, Plasma nitriding of 316L austenitic stainless steel: Experimental investigation of fatigue life and surface evolution, *Surf. Coat. Tech*. 204 (2010) 1947-1951.

K. Gemma, T. Obtruka, T. Fujiwara, M. Kwakami, Prospects for rapid nitriding in high Cr austenitic alloys, in *Stainless Steel 2000*, p159-166, Ed. Tom Bell and Katruya Akamatsu, Maney Publishing, Leeds, 2001.

K.-T. Rie, E. Broszeit, Plasma diffusion treatment and duplex treatment — recent development and new applications, *Surf. Coat. Tech*. 76–77 (1995) 425-436.

Li, X. Y. and Dong, H.: *Effect of annealing on corrosion behaviour of nitrogen S phase in austenitic stainless steel*, Materials Science and Technology (2003) 19, *10,* 1427-1434.

M. Tsujikawa, D. Yoshida, N. Yamauchi, N. Ueda, T. Sone, S. Tanaka, Surface material design of 316 stainless steel by combination of low temperature carburizing and nitriding, *Surf. Coat. Tech.* 200 (2005) 507-511.

M. Tsujikawa, S. Noguchi, N. Yamauchi, N. Ueda and T. Sone, Effect of molybdenum on hardness of low-temperature plasma carburized austenitic stainless steel, *Surf. Coat. Tech*. 201 (2007) 5102-5107.

Martin, W. C. and Wiese, W. L.: *Atomic, molecular, and optical physics handbook* in 2.1st Ed. (2002) Gaithersburg, NIST,

Parrish, G. and Harper, G. S.: *Production gas carburizing*, 1st Ed. (1985) Oxford, Pergamon

Reynoldson R.W, Advances in surface treatments using Fluidized beds, *Surface and Coatings Technology.*, Vol. 71; 2, pp. 102-107, 1995.

Somers, M.A.J, Christiansen, T., and Møller, P. Case-hardening of stainless steel European Patent 1521861 (2004) EU.

Somers, M.A.J., and Christiansen, T., (2005) Kinetics of microstructure evolution during gaseous thermochemical surface treatment. *J. Phase Equilibria and Diffusion*, No. 5, vol. 26, p. 520-528.

Standard British Standard EN 10052:1994, Vocabulary of heat treatment terms for ferrous products, BSI, London, www.bsi-global.com

Sun, Y. and T. Bell.: *Plasma surface engineering of low alloy steel*, Materials Science and Engineering A: Structural Materials: Properties, Microstructure and Processing (1991) A140, 419-434

T. Bell and Y. Sun, Low temperature plasma nitriding and carburizing of austenitic stainless steels, *Heat Treatment of Met*als 29 (3) (2002) 57-64

T. Bell, *Bodycote-AGA* Seminar, Lidingö, 2005.

T. Czerwiec, Presentation in International Symposium on Surface Hardening Corrosion Resistant Alloys – ASM, Case Reserve Western University, Cleveland, Ohio USA. May, 2010.

Thaiwatthana, S., Li, X. Y., Dong, H. and Bell, T.: *Comparison studies on properties of nitrogen and carbon S phase on low temperature plasma alloyed AISI 316 stainless steel*, Surface Engineering (2002) 18, *6,* 433-437

Thaiwatthana, S., Li, X. Y., Dong, H. and Bell, T.: *Corrosion wear behaviour of low temperature plasma alloyed 316 austenitic stainless steel*, Surface Engineering (2003) 19, *3,* 211-216

X.Y. Li, J. Buhagiar, H. Dong, Characterisation of dual S phase layer on plasma carbonitrided biomedical austenitic stainless steels, *Surf. Eng*. 26 (2010) 67-73.

Y. Sun and E. Haruman, Influence of processing conditions on structural characteristics of hybrid plasma surface alloyed austenitic stainless steel, *Surf. Coat. Tech.* 202 (2008) 4069-4075.

Y. Sun and T. Bell.: *Dry sliding wear resistance of low temperature plasma carburised austenitic stainless steel*, Wear (2002) 253, *5-6,* 689-693

Y. Sun and T. Bell.: *Effect of layer thickness on the rolling-sliding wear behavior of low- temperature plasma-carburized austenitic stainless steel*, Tribology Letters (2002) 13, *1,* 29-34

Y. Sun, Kinetics of low temperature plasma carburizing of austenitic stainless steels, *J. Mater. Proc. Tech.* 168 (2005) 189-194.

Y. Sun, X.Y. Li and T. Bell, Low temperature plasma carburizing of austenitic stainless steels for improved wear and corrosion resistance, *Surf. Eng*. 15 (1999) 49-54.

Y. Sun, X.Y. Li and T. Bell, X-ray diffraction characterisation of low temperature plasma nitrided austenitic stainless steels, *J. Mater. Sci.* 34 (1999) 4793-4802

Corrosion Resistance

Edited by Dr Shih

ISBN 978-953-51-0467-4
Hard cover, 472 pages
Publisher InTech
Published online 30, March, 2012
Published in print edition March, 2012

The book has covered the state-of-the-art technologies, development, and research progress of corrosion studies in a wide range of research and application fields. The authors have contributed their chapters on corrosion characterization and corrosion resistance. The applications of corrosion resistance materials will also bring great values to reader's work at different fields. In addition to traditional corrosion study, the book also contains chapters dealing with energy, fuel cell, daily life materials, corrosion study in green materials, and in semiconductor industry.

InTech Europe
University Campus STeP Ri
Slavka Krautzeka 83/A
51000 Rijeka, Croatia
Phone: +385 (51) 770 447
Fax: +385 (51) 686 166
www.intechopen.com

InTech China
Unit 405, Office Block, Hotel Equatorial Shanghai
No.65, Yan An Road (West), Shanghai, 200040, China
中国上海市延安西路65号上海国际贵都大饭店办公楼405单元
Phone: +86-21-62489820
Fax: +86-21-62489821